

FIGURE LEGENDS

Fig. S1. Kinetics of PCNA opening. Opening of PCNA-WC^{AEDANS} was measured as described in Fig. 2A, except at higher RFC concentration (final concentrations: 2 μ M RFC, 0.25 μ M PCNA and 0.5 mM ATP). A 2-exponential fit of the data yields $k_{\text{open}(1)} = 2.5 \text{ s}^{-1}$ and $k_{\text{open}(2)} = 0.6 \text{ s}^{-1}$.

Fig. S2. DNA binding to RFC measured under various conditions. (A) ptDNA_{TAMRA} (5 nM) and ssDNA_{TAMRA} (5 nM, 5'-labeled 55-nt ssDNA) were titrated with RFC (0 – 50 nM) in the presence of ATP γ S (0.1 mM) and PCNA (200 nM) in buffer A. The fluorescence signal (normalized to free DNA) was plotted *versus* RFC concentration, and the data fit to a quadratic function yielded $K_D \leq 1 \text{ nM}$ for both DNA substrates. (B) Kinetics of ptDNA_{TAMRA} binding/release measured as in Fig. 3A, at Δt : 0.02 and 3s, except with higher protein concentrations (final concentrations: 0.1 or 1 μ M RFC, 3 μ M PCNA, 0.04 μ M ptDNA_{TAMRA} and 0.5 mM ATP). The exponential binding rate is 17 s^{-1} at 1 μ M RFC, Δt : 3s. (C) Kinetics of ptDNA_{TAMRA} binding measured as in Fig. 3A, at Δt : 10s, except with ATP γ S instead of ATP in the reaction (final concentrations: 0.1 RFC, 0.4 μ M PCNA, 0.04 μ M ptDNA_{TAMRA} and 0.1 mM ATP γ S). The relative change in ptDNA_{TAMRA} fluorescence intensity on binding RFC•ATP γ S•PCNA is 1:2.1 (from A, C).

Fig. S3. Data from Fig. 5 shown on a log scale for time. (A) Overlay of data from PCNA opening/closing, DNA binding/release, ATP hydrolysis and Pi release experiments provides a visual of rapid ptDNA binding to RFC•ATP•PCNA complex (formed during pre-incubation, Δt :

3 s) triggering ATP hydrolysis, PCNA closure, Pi release, PCNA•ptDNA dissociation and catalytic turnover. Data for (B) PCNA opening (Δt : 0.1, 7 s), (C) PCNA opening/closing, (D) ptDNA binding/release, (E) ATP hydrolysis (Δt : 2 s), and (F) Pi release (only Δt : 0.02, 0.2, 2 s shown in C, D, F for clarity), were all fit simultaneously to the model shown in Scheme I. The black lines are simulations generated by the model based on parameters listed in Table I.

Fig. S4. Confidence contour analysis. Confidence contours for the global fit to rate constants derived by simultaneously fitting all the data to the model in Scheme I. All 6 pair wise combinations of the 4 unknown rate constants: k_2 (linked with k_{-2} , k_3 , k_{-3} , k_4), k_8 , k_{11} , k_{12} (linked with k_{-12}) are shown. The central red zone shows the area of good fit. The yellow band between the red and green zones delineates a 10% increase in χ^2 value, which was used to estimate the upper and lower confidence limits on each kinetic parameter listed in Table I.

Fig. S5. DNA dependence of RFC-catalyzed ATP hydrolysis and Pi release. RFC-catalyzed Pi release is measured by change in fluorescence intensity of MDCC-PBP. Pre-incubation of RFC, PCNA with ATP (Δt : 2 s) followed by addition of ptDNA results in a burst of Pi release followed by a linear steady state phase. In contrast, no burst phase is detectable with ssDNA, only a linear rate of $1.1 \mu\text{M s}^{-1}$.

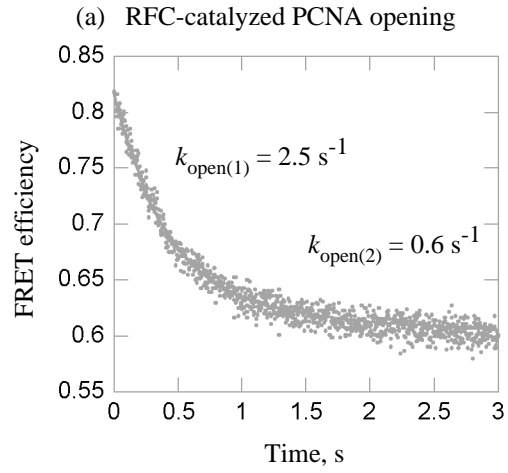
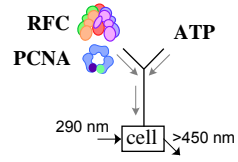
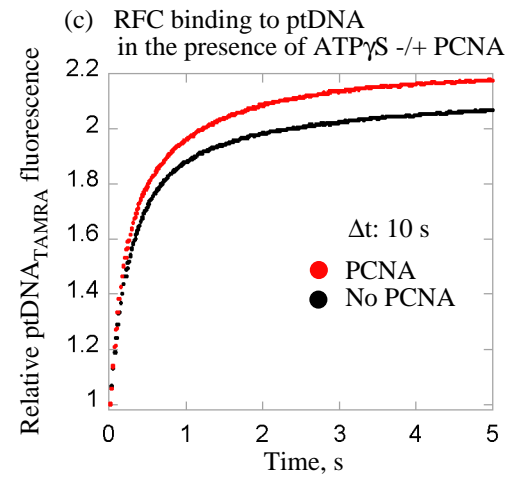
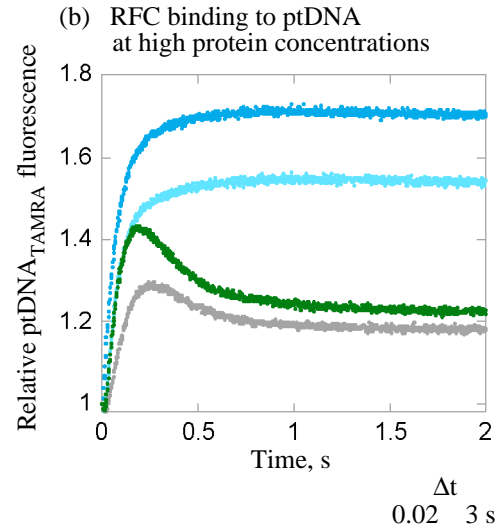
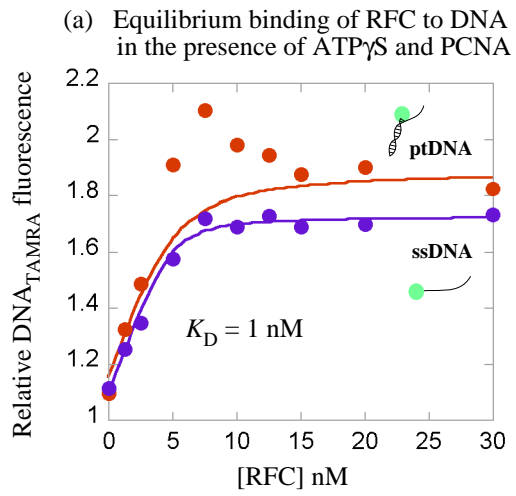
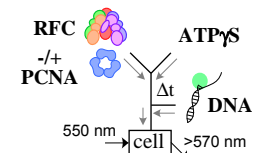
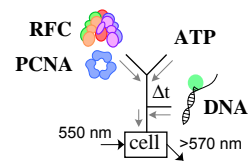


Figure S1



Δt
 0.02 3 s
 [RFC] 0.1 μ M, [PCNA] 3 μ M ● ●
 [RFC] 1 μ M, [PCNA] 3 μ M ● ●

Figure S2

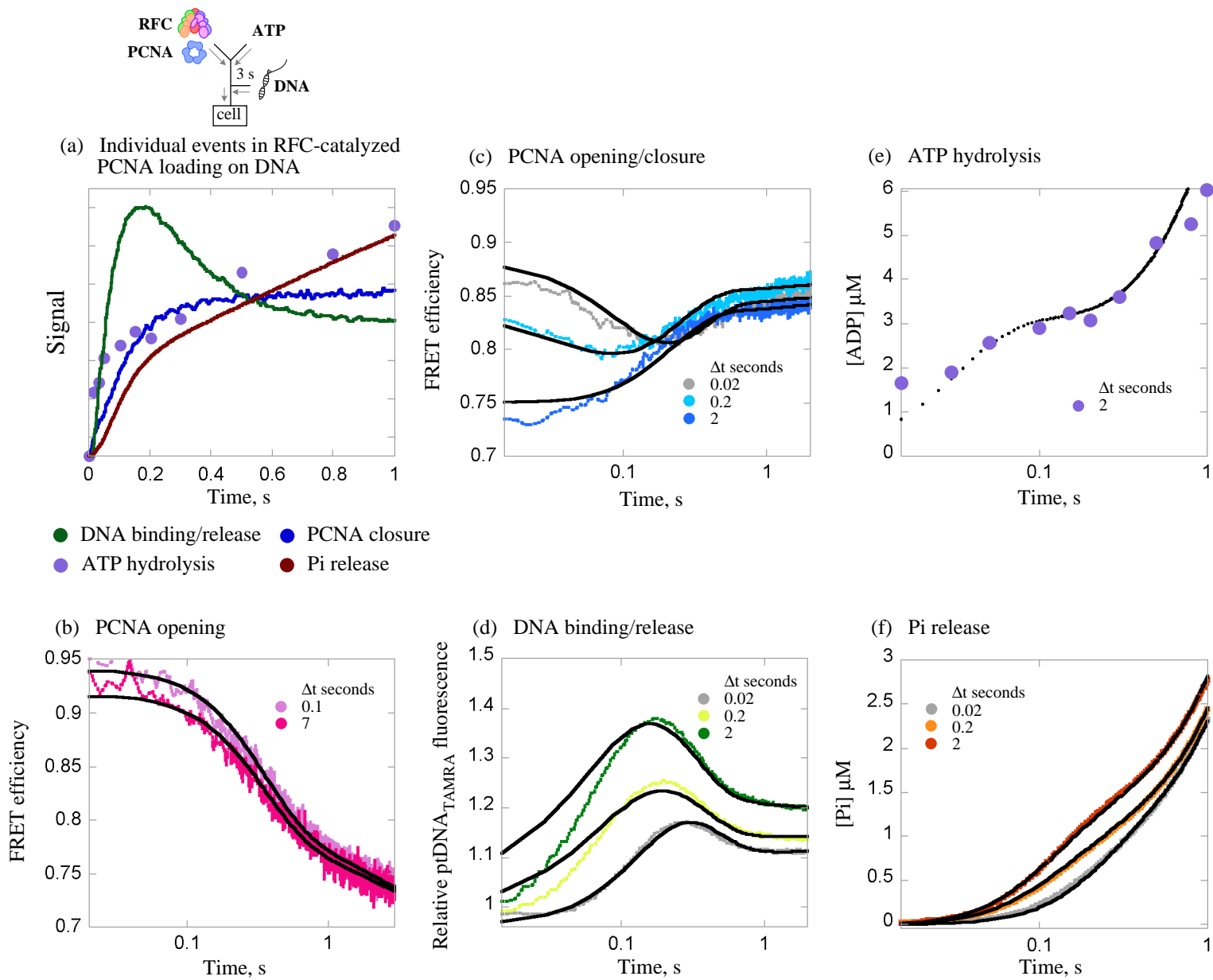


Figure S3

Confidence contours for unknown rate constants derived from global fitting of kinetic data to a minimal model (Scheme I)

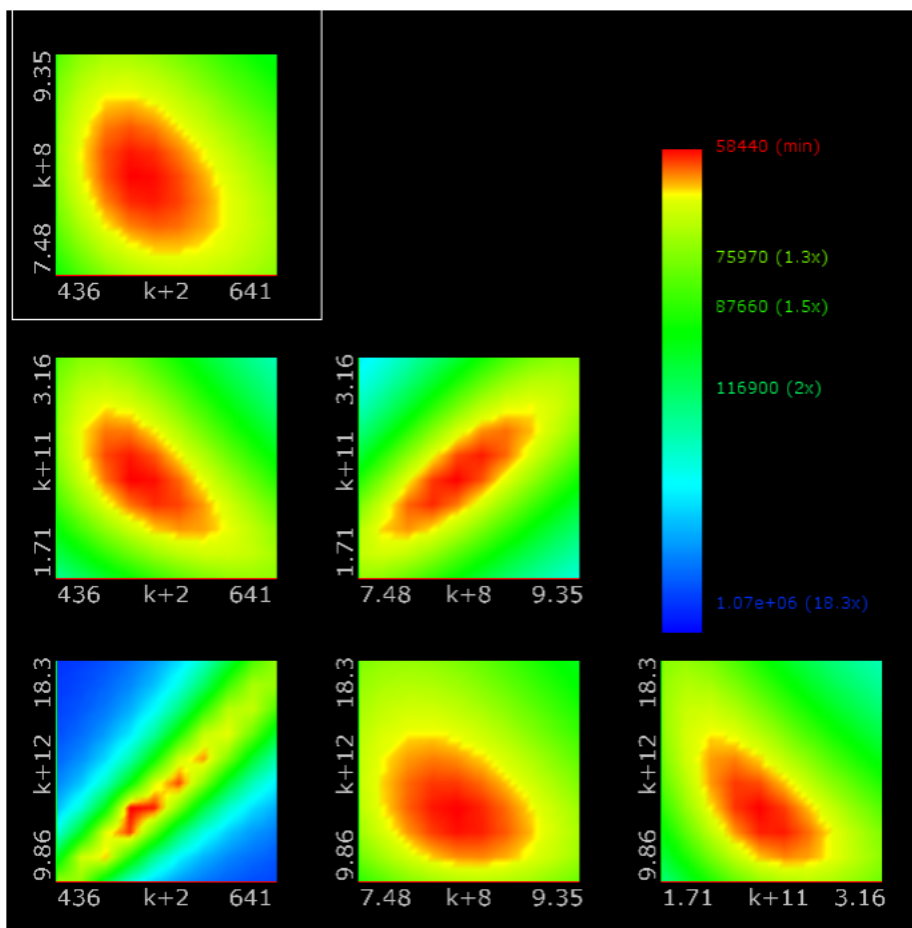
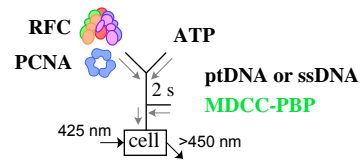


Figure S4



RFC-catalyzed ATP hydrolysis and phosphate (Pi) release

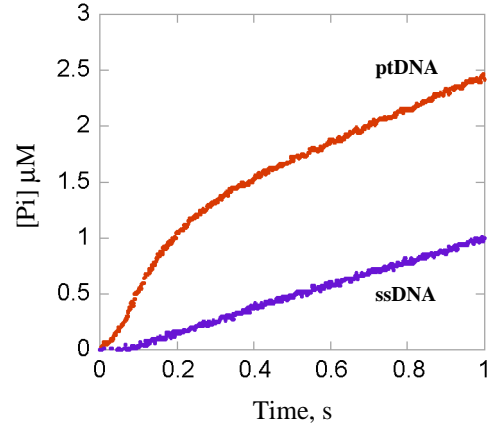


Figure S5